



EFFECT OF CHEMICAL MODIFICATION OF TITANIUM DIOXIDE PARTICLES VIA SILANIZATION UNDER PROPERTIES OF CHITOSAN/POTATO-STARCH FILMS

EFFECTO DE LA MODIFICACIÓN QUÍMICA DE LAS PARTÍCULAS DE DIÓXIDO DE TITANIO MEDIANTE SILANIZACIÓN SOBRE LAS PROPIEDADES DE LAS PELÍCULAS DE CHITOSAN/ALMIDÓN DE PAPA

J.A. Gonzalez-Calderon¹, J. Vallejo-Montesinos², H.N. Martínez-Martínez³, R. Cerecero-Enríquez³,
L. López-Zamora^{3*}

¹ CONACYT-Instituto de Física, Universidad Autónoma de San Luis Potosí (IF-UASLP), Alvaro Obregón 64, 78000 San Luis Potosí, SLP México.

² División de Ciencias Naturales y Exactas, Campus Guanajuato Departamento de Química, Universidad de Guanajuato, Guanajuato Guanajuato 36050, México.

³ División de Estudios de Posgrado e Investigación, Tecnológico Nacional de México, Instituto Tecnológico de Orizaba, Av. Oriente 9 No. 852. Col. Emiliano Zapata C.P. 94320, Orizaba, Veracruz México.

Received: November 8, 2018; Accepted: January 11, 2019

Abstract

In this work we present a simple way to improve the dispersion of titanium dioxide (TiO₂) particles inside chitosan/potato-starch films by chemical modification of the surface of these nanoparticles via silanization. The films increased in luminosity due to the modified particles, in addition to the fact that the water activity remained within the acceptable values for microbial non-proliferation. The thermal analyzes indicated that the addition of TiO₂ increases the glass transition temperature in the film, and the addition of functional groups such as those of the silane, give mobility to the polymer chains during the rise in temperature. The mobility of the polymer is related to a decrease in the value of the temperature necessary to reach a vitreous state in the films that contains silanized particles. The most important result was that the existence of these functional groups reduced the enthalpy of decomposition of the films making them more stable for thermal degradation. The photo-oxidation results suggested the passivate of TiO₂ thanks to the presence of silane, which implies that it is a more stable film against UV radiation, avoiding the negative effect of unmodified TiO₂ particles.

Keywords: chitosan, potato-starch, titanium dioxide, 3-aminopropyltriethoxysilane.

Resumen

En este trabajo se presenta una manera sencilla de mejorar la dispersión de partículas de dióxido de titanio (TiO₂) en películas de almidón-quitosán mediante la modificación química de la superficie de estas nanopartículas vía silanización. Las películas aumentaron de luminosidad debido a las partículas modificadas, además la actividad de agua permaneció dentro de valores aceptables para la no proliferación microbiana. Los análisis térmicos indicaron que la adición de TiO₂ incrementa la temperatura de transición vítrea en la película, y la adición de grupos funcionales como el silano, otorgan movilidad a las cadenas poliméricas durante el ascenso de temperatura. La movilidad del polímero está relacionada al decremento en el valor de temperatura necesaria para alcanzar el estado vítreo en las películas que contienen partículas silanizadas. La contribución más importante fue que la existencia de estos grupos funcionales reduce la entalpía de descomposición de las películas haciéndolas más estables para la degradación térmica. Los resultados de la foto-oxidación sugieren la pasivación del TiO₂ gracias a la presencia del silano, lo cual implica que es una película más estable frente a las radiaciones UV, evitando el efecto negativo de las partículas de TiO₂ sin modificar.

Palabras clave: quitosán, almidón de papa, dióxido de titanio, 3-aminopropiltriétoxisilano.

* Corresponding author. E-mail: letylopezito@gmail.com

<https://doi.org/10.24275/uam/izt/dcbi/revmexingquim/2019v18n3/GonzalezC>
issn-e: 2395-8472

1 Introduction

The excessive number of products that are discarded every day, has caused great concern at present. The focus main being related to the conventional synthetic plastic materials derived from petroleum. This reality is the main reason for the research in order to develop new materials of biodegradable packaging, such as those derived from renewable resources, such as polysaccharides, proteins and lipids, since they combine environmental criteria and sustainability, with chitosan and starch being the polysaccharides of greatest interest (Dias *et al.*, 2010, Xu *et al.*, 2005, Vázquez *et al.*, 2009, Dang and Yoksan 2016, Jiang *et al.*, 2016, Zhou *et al.*, 2016, Bergel *et al.*, 2017, Volpe *et al.*, 2017).

Chitin is the second most abundant biopolymer in nature after cellulose. Chitosan is the deacetylated form of chitin, it is a copolymer formed by 2-deoxy-2-amino-anhydroglucose, with less than 40% deacetylation and which, in most cases, will be soluble in acids (Volpe *et al.*, 2017, Zhai *et al.*, 2004, Chakrabarty *et al.*, 2010, Arockianathan *et al.*, 2012, Praxedes *et al.*, 2012, Perez and Francois, 2016). In an acidic environment, the amino group (-NH₂) of chitosan can be protonated in NH₃⁺ and easily form electrostatic interactions with anionic groups in an acidic environment, the property of which has been applied in edible films (Xu *et al.*, 2005, Volpe *et al.*, 2017).

Chitosan offers a wide potential that can be applied to the food industry due to its particular physicochemical properties, such as biodegradability, biocompatibility with human tissues, non-toxic and especially its antimicrobial and antifungal properties. These aspects make it of vital interest for the preservation of food and emerging technologies (Volpe *et al.*, 2017, Zhai *et al.*, 2004, Tripathi *et al.*, 2009, Bajer and Kaczmarek, 2010, Hari and Nair, 2016, Li *et al.*, 2016). Although chitosan films are highly impermeable to oxygen, they have relatively little water vapor. The functional properties of chitosan films are improved when chitosan is combined with other film-forming materials (Xu *et al.*, 2005, Santacruz *et al.*, 2015).

Starch, on the other hand, is a polymer composed of amylose and amylopectin, is abundant, biodegradable, edible, renewable and inexpensive (Perez and Francois, 2016; Bourtoom and Chinnan, 2008; Mei *et al.*, 2013; Silva-Weiss *et al.*, 2013;

Ostafińska *et al.*, 2017). However, the wide application of starch film and its use as a native form has been restricted by some limitations in specific applications due to its water solubility and fragility (Xu *et al.*, 2005, Dang and Yoksan, 2016, Bourtoom and Chinnan, 2008), therefore, like chitosan, the starch films are mixed with different proteins to decrease the water vapor permeability and increase their tensile strength (TS). The interest in combining polysaccharides, proteins and lipids is due to the advantages and disadvantages of these components, significantly changing the physical and rheological properties (Dias *et al.*, 2010; Xu *et al.*, 2005; Vázquez *et al.*, 2009; Zhou *et al.*, 2016; Silva-Weiss *et al.*, 2013; López *et al.*, 2017).

The introduction of nanometric particles in a polymeric matrix is a strategy that is widely used to produce hybrid materials with specific properties, especially to solve the low mechanical resistance of polymers obtained from natural sources (Hamdi *et al.*, 2015; Hamden *et al.*, 2016). One of the alternatives is to look for compounds that have affinity for the amino and hydroxyl groups in chitosan, which have been shown to have affinity for cations through electrostatic attraction or ion exchange (Handem *et al.*, 2016; Hadi-Najafabadi *et al.*, 2015; Razzaz *et al.*, 2016). This is how, by means of different nanostructures, the polymers can present different values of permeability to gases and water vapor, to meet the preservation requirements of drugs, fruits, vegetables, beverages, etc. Polymeric materials with greater resistance to light, better mechanical, rheological and thermal properties can also be obtained. These modifications in the materials can mean increases in the storage time of the product, less loss of chemical, physical and organoleptic characteristics, as well as facilitating transport (Lian *et al.*, 2016).

Among the materials that are included in the category of nanometric particles is titanium oxide (TiO₂), which has called the interest in many industrial fields, but recently in the environmental and medical fields as an antibacterial and antifungal agent. TiO₂ is a semiconductor sensitive to light that absorbs electromagnetic radiation, mainly in the UV region; It is also an amphoteric oxide, which is very chemically stable. Due to the aforementioned characteristics, it is the most commonly used photocatalyst to degrade organic molecules during water purification, as well as for filling in polymer matrices. In addition, it is used in paints, pigments, anticorrosive and glass coatings, gas sensors, production of electrodes for electrochemistry, solar cells, UV absorbers, in cosmetic products and

generally in the ceramics industry (Lian *et al.*, 2016, Furuzono *et al.*, 2003, Bozzi *et al.*, 2005, Daoud *et al.*, 2005, Ochoa *et al.*, 2010, Sreekumar *et al.*, 2012, Xiao *et al.*, 2015, Shirakawa *et al.*, 2016). as well as a wide variety of materials, especially for those with low heat resistance such as textiles, wood, plastics, papers and biomaterials (Daoud *et al.*, 2005, Mihailović *et al.*, 2010). However, it has a polar surface, while the polymer matrix is not polar, which makes the surface adhesion between the matrix and the TiO₂ deficient (Soto *et al.*, 2014, Zarazua *et al.*, 2017, Estrada *et al.*, 2016). To improve its stability, a surface agent is required, such as 3-aminopropyltriethoxysilane (APTES), which is coupled to TiO₂ by a silanization process (Perez and Francois 2016, Ostafińska *et al.*, 2017, Hamdi *et al.*, 2015, Handem *et al.*, 2016, Hadi-Najafabadi *et al.*, 2015, Razzaz *et al.*, 2016, Solís-Gómez *et al.*, 2014, Meroni *et al.*, 2017, Ahmad *et al.*, 2017, Liu *et al.*, 2015, Weerachawanasak *et al.*, 2015, Ostwal *et al.*, 2011). By incorporating functionalized TiO₂ nanoparticles into polymer matrices, there is an improvement in the mechanical properties, such as tensile strength, elongation at break, this is due to the formation of chemical bonds between the functional groups of coupling agent and the polymers (Lian *et al.*, 2016, Sreekumar *et al.*, 2012, Huang *et al.*, 2017). In previous investigations such as the one conducted by Shiraishi *et al.*, 2014, the hydrophobic character of the siloxane formed on the surface of the TiO₂ nanoparticles helps the 2,4-DNP (hydrophobic) molecules to integrate under the amino groups and thus carry out the photodegradation process. In this work, TiO₂ nanoparticles previously functionalized were incorporated to chitosan/potato-starch films which have a polar character as a whole. Due to this hydrophilic nature of the mixture, the polymer chains bind to the particles on the outside (amino groups) thus causing the electron movement to take place in the hydrophobic part (siloxane). Improving the photocatalytic stability of the particles and avoiding photodegradation and also, improving their mechanical properties, demonstrating that the chemical modification allows the titanium dioxide particles to be properly dispersed within the polymeric matrix.

These results are useful for the development and improvement of materials based on natural sources and look for an alternative to synthetics as secondary packaging material. In addition, it was demonstrated by means of the chemical modification with APTES the stability to the degradation induced by the UV radiation is improved, which is one of the adverse

phenomena that is had in the composites with titanium dioxide.

2 Methodology

2.1 Silanization of TiO₂ nanoparticles

For TiO₂ functionalization, different proportions were used of TiO₂:APTES, ethanol was used as the reaction medium, 30 min of magnetic stirring at 350 rpm were interspersed, with 30 min of sonication at 40 KHz in an ultrasonic bath, finally reaching a total of 2.5 h. Subsequently, the APTES was added and in a 10-min interval 1 mL of water was added to promote hydrolysis in the reaction and left under agitation at 400 rpm for 6 more hours. Washes were performed twice with distilled water and five times with methanol at 3000 rpm, this was done by centrifugation for 10 min for each wash, this was to remove agents that have not reacted. The drying was carried out in an oven at 80 ° C for 3 h. The dry powders were stored in vials for further tests.

2.2 Film-forming

The film-forming solution (FFS) was made in a 1: 1 ratio of chitosan: starch. 200 mL of lactic acid solution (1% v/v) was prepared, 6 g of chitosan (3% w/v) were added, stirring at 650 rpm for 13 h. For the sol of the starch, 200 mL of distilled water was used, stirring at 400 rpm, heating at 75°C until reaching the point of gelatinization. It was brought to room temperature and incorporated in the chitosan sol, adding glycerol as a plasticizer to 25% by weight of total solids. The FFS was poured into acrylic plates, performing a forced convection drying at 55 °C for 6 h and then at room temperature to complete 48 h. The films were stored for later tests.

The nanoparticles were first incorporated into a lactic acid solution (1% v/v) by magnetic stirring for 3 h, then the chitosan was added to make the sol, and the same procedure described above was followed for the production of films, but with different samples of NPs.

2.3 Characterization of films

The biofilms were characterized by means of the following tests: color, thickness, water activity (aw) structural analysis (FTIR, WAXD, SEM), thermal analysis (DSC) and mechanical tests (Young's modulus, tensile strength and elongation to break).

The color readings of the films were made using a Chroma Meter colorimeter, model CR-400, Minolta Konica, using the CIE L* a* b* color space (CIELAB) and the corresponding scales for the L parameters (between 100 (white) to 0 (black)), for a* and b* + a (red) to -a (green), + b (yellow) to -b (blue) respectively (Bourtoom and Chinnan, 2008, Silva-Pereira *et al.*, 2015).

The thickness of the films was measured using a digital Vernier Calibrator Electronic Digital Caliper, with a sensitivity of 0.01 mm, for this purpose samples were cut at random places. The measurement was made in triplicate.

A Decagon Aqualab digital hygrometer was used to evaluate the a_w of the films. In the cells of the instrument, circular samples of the films were placed, taking into account that the bottom of the cell was covered with the sample.

Mechanical tests were performed on tensile strength and elongation to break (TS and E respectively), which were carried out with the help of a texture analyzer (texturometer) Stable Micro Systems model TA.XT plus. For the calculation of the Elongation at Break (% E) Equation 1 was used, with the data provided of the stress-strain curves, in units of distance.

$$\%E = \left[\frac{L - L_0}{L_0} \right] \times 100 \quad (1)$$

where L = final length, L_0 = initial length, $\%E$ = Elongation at break.

For the structural analysis, the Perkin-Elmer FTIR-ATR spectrometer was used to identify the compounds present in the ten types of films formed. The analysis was performed in a range of 4000 to 600 cm^{-1} and 60 scans per spectrum. The original and baseline spectra were exported at the end of each reading. The X-ray patterns of the films were obtained using a PANalytical X-ray diffractometer model X'Pert PRO, using radiation $\text{CuK}\alpha = 1.54056 \text{ \AA}$. The scans were performed between $2\theta = 20$ to 50° with a speed of $4^\circ/\text{min}$ and the morphological analysis was performed using a scanning electron microscope JEOL JSM 6060 operating under high vacuum.

Samples of $4 \times 2 \text{ cm}$ of the films were exposed to a UV radiation for 42 days, and during this time infrared analysis was carried out at random times to determine the changes produced by UV light in the spectra of the films.

Table 1. Functionalized nanoparticles and their ratio TiO_2 :APTES.

| Route | Sample | TiO_2 (g) | APTES (mL) |
|-------|--------|--------------------|------------|
| 1 | M1 | 0.5 | 1 |
| 2 | M2 | 1 | 1 |
| 3 | M3 | 5 | 1 |
| 4 | M4 | 10 | 1 |

Table 2. Chitosan/potato-starch films with silanized NPs and their reference simples.

| Film | | Nanoparticles | |
|----------|-------|---------------|--|
| Sample | Route | Sample | |
| C | - | - | |
| T | 0 | T | |
| 1-M1-CPS | 1 | M1 | |
| 1-M2-CPS | 2 | M2 | |
| 1-M3-CPS | 3 | M3 | |
| 1-M4-CPS | 4 | M4 | |

3 Results and discussion

From the nanoparticle functionalization process carried out by López-Zamora *et al.* (2018), four routes were obtained, which are presented in Table 1 with their respective nomenclature. Where the difference lies in the TiO_2 /APTES ratio that is used during the modification process.

Chitosan/potato-starch films were made at 1% by weight of the NPs of Table 1, named as shown in Table 2, where CPS refers to the film's polymers (Chitosan/Potato-Starch) without no type of titanium dioxide particle filler. These films were characterized by different techniques, such as mechanical tests, differential scanning calorimetry (DSC), colorimetry, water activity, and scanning electron micrographs.

3.1 Effect of the ratio APTES/ TiO_2 on the properties of chitosan/potato-starch films

The physicochemical characterization was carried out, within the evaluation of the properties of the films, considering their mechanical behavior, color and water activity. The results of these measurements are summarized in Table 3.

Table 3. Colorimetric analysis, aw, thickness and mechanical properties of the chitosan/potato-starch films.

| Sample | a_w | L | a^* | b^* | Thickness (μm) | Young's modulus (MPa) | Tensile strength (MPa) | Elongation at break (%) |
|-----------------|-------|-------|-------|-------|-----------------------------|-----------------------|------------------------|-------------------------|
| C | 0.27 | 30.51 | -0.17 | 1.43 | 73 | 333.7 | 20.27 | 29 |
| T | 0.27 | 51.22 | -2.17 | 2.56 | 93 | 348.13 | 20.76 | 37 |
| 1-M1-CPS | 0.28 | 51.58 | -2.35 | 2.83 | 70 | 67.1 | 14.87 | 71 |
| 1-M2-CPS | 0.28 | 49.73 | -2.1 | 1.1 | 67 | 253.13 | 15.25 | 32 |
| 1-M3-CPS | 0.29 | 48.08 | -1.9 | 1.4 | 70 | 237.96 | 18.06 | 45 |
| 1-M4-CPS | 0.31 | 45.93 | -1.71 | 2.32 | 100 | 215 | 13.25 | 41 |

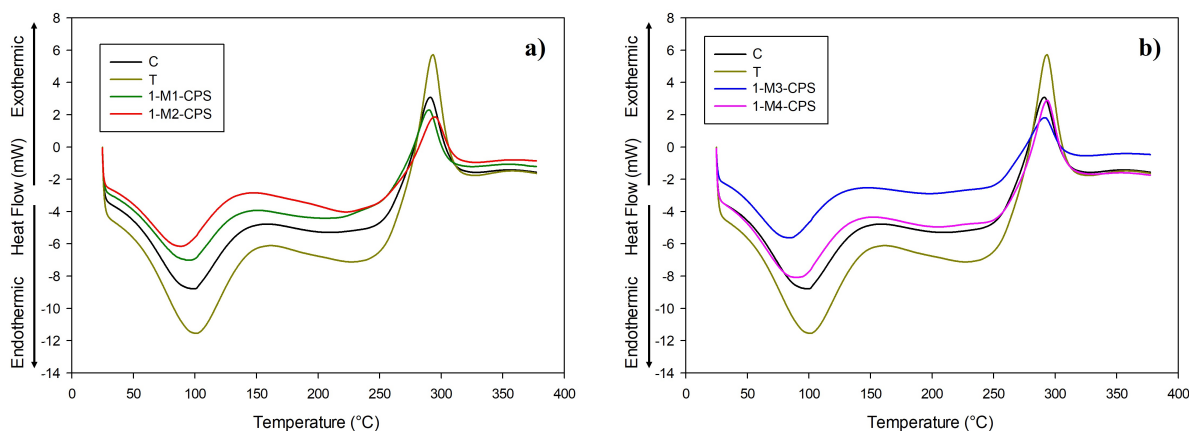


Fig. 1. DSC thermograms of the control film C, film T and its comparison with a) film 1-M1-CPS and 1-M2-CPS, b) film 1-M3-CPS and 1-M4-CPS.

As it is known, a high value of Young's modulus (also called modulus of elasticity) indicates greater rigidity of the material, on the opposite side, a material will be soft when it has a smaller Young's modulus (Sreekumar *et al.*, 2012). Firstly, comparing the control film C with the film T containing titanium dioxide without modification with the APTES agent, this film showed an increase of 10.22% in the Young's modulus which indicates that the addition of the TiO_2 nanoparticles in the film polymeric will make it more rigid with respect to the first. The TS value of the control film C was 20 ± 2 MPa, similar to the value obtained by Volpe *et al.*, (2017), who reported a TS value of 19 ± 2 MPa for a film formed by sodium caseinate and chitosan in the proportion 1:1. However, the tensile strength (TS) and elongation at break (% E) also resulted in an increase in the film with NPs, this verifies what is stated in the literature, that the addition of TiO_2 in polymers improves the properties mechanical of these. The study conducted by Sreekumar *et al.*, (2012), provided a TS value of 15.3 ± 0.4 MPa at 1% by weight of TiO_2 , however,

the film they made was starch with polyvinyl alcohol, while Jiang *et al.*, (2016) obtained an improvement of TS from 8.8 to 15 MPa in pea starch films when they incorporated NPs of potato starch.

Another important parameter, is the thermal behavior of the material with of a rise in temperature, differential scanning calorimetry was used to analyze said characteristic, Fig. 1 represents the DSC thermograms of the samples analyzed and the glass transition temperature can be identified (glass transition temperature, T_g) of the films, different values of T_g have been reported for chitosan, but in the presence of water values of 61°C have been obtained (Sarwar *et al.*, 2015, Dhawade and Jagtap, 2012), in the present work, it was obtained that the films C and T reached a T_g in approximate values of 67°C and 69°C respectively, the control film had a value of T_g close to that of chitosan, but a little high due to the presence of starch. The temperature increase of 2°C of the film with NPs was attributed to the chains of the polymeric matrix having less mobility caused by the incompatibility of the inorganic NPs with the

polymers, since more temperature is necessary to cause a free movement between the polymer chains (Zhang *et al.*, 2016).

One of the physicochemical characteristics of high impact for consumer acceptance is color. The results obtained from the measurements were expressed according to the CIE $L^* a^* b^*$ color system (Bourtoom and Chinnan, 2008; Silva-Pereira *et al.*, 2015). Table 3 shows the colorimetry data made to the films. It was evident that the film with TiO_2 (sample T) will increase its luminosity, since the TiO_2 is used as a pigment, this increased the parameter L^* with respect to the film C, in the same way for the other rectangular coordinates, T tended to be greener and more yellow, by the nature of the pigmentation. The study carried out by Oleyaei *et al.*, (2016) on the properties of its potato starch films with 1% by weight TiO_2 , the L^* parameter (51.14) was very similar to the one obtained in this investigation, however, the parameters a^* and b^* changed very drastically with respect to this work, since the films they made were only composed of potato starch, probably the absence of chitosan caused the results of these parameters to differ from those presented in Table 3.

The films with functionalized NPs were also analyzed, these samples had incorporated 1% by weight of TiO_2 of the different proportions according to what is shown in Table 1. The effects that caused the existence of organic groups on the surface of the NPs were changes remarkable in the results of the mechanical tests, as shown in Table 3. In the film 1-M1-CPS the modulus of elasticity and TS decreased, indicating that the film was more elastic, and can be corroborated in the data of elongation at break of up to 71% against 37% of the sample with NPs without functionalization, approximately twice the elongation, since the more rigid it is, the less it will elongate and vice versa.

The T_g of the films with silanized NPs were 64, 60, 57 and 63 °C respectively, in this case, the temperature tended to decrease with each one of the samples, they were 3 to 10 °C lower than the control film C, the decrease was attributed to the presence of APTES functional groups that gave "mobility" of the polymer chains, a chain that can be easily mobilized, will have a low T_g , while one that does not move as much, will have a high T_g . The more easily a polymer can move, the less heat will have to be supplied for the chains to begin to contour to leave a rigid vitreous state and move to another soft and flexible, in addition to a compatibility by the formation of hydrogen bonds between the TiO_2 and the polymers (Lian *et al.*, 2016)

and consequently the T_g decreased. The sample 1-M4-CPS unlike the other three films, instead of decreasing its T_g , exhibited an increase, but still being less than the control film and probably due to the existence of less amount of APTES present in the TiO_2 surface due to the proportions used in the silanization path of these NPs. The endothermic peaks included in the range of 85 to 100 °C shown by the films are attributed to the loss of water, and represent the energy needed to evaporate the water absorbed in the film (Tripathi *et al.*, 2009). According to this, the film T had a greater amount of water absorbed during the analysis procedure, hence the description of a greater endothermic peak.

In addition to the glass transition temperature, in the curves of calorimetric analysis an exothermic peak is observed at 290 °C, which was present in all the samples, which indicates the thermal degradation of the films (Tripathi *et al.*, 2009), however, not all of them had the same heat flow. The film with TiO_2 without functionalization described a greater peak than the control sample C, but the peaks described by the films with silanized TiO_2 were slightly lower in intensity than the reference films, except for 1-M4-CPS (Fig. 1b). The existence of the coupling agent APTES on the surface of TiO_2 influences the thermal analysis of the films, the decomposition temperature is practically not affected, however, the enthalpy of the decomposition of the film is reduced, which shows that the APTES reduces the heat generated in the decomposition of the blend chitosan/potato-starch, thus giving a greater thermal stability to the film (Kimura *et al.*, 2016). The similar behavior of 1-M4-CPS with C, is probably due to the fact that the NPs of said film had a smaller amount of coupling agent, due to this, the enthalpy tended to increase until describing a curve like the control film, however, the minimal present quantity of APTES caused that the thermogram peak of 1-M4-CPS did not have the intensity that the film T.

The incorporation of organic groups of the APTES also showed changes in the colorimetry of the films with NPs functionalized at the concentration of 1% by weight, firstly, 1-M1-CPS had a slight increase in the three parameters, indicating that the agent APTES influenced in color, but imperceptibly, the proportions of the APTES content in the NPs of the following films caused the parameters to tend to decrease, although they were all at 1%, they showed lower green and yellow tones, as well as luminosity, deducting with this that the APTES interferes with the colors of the films.

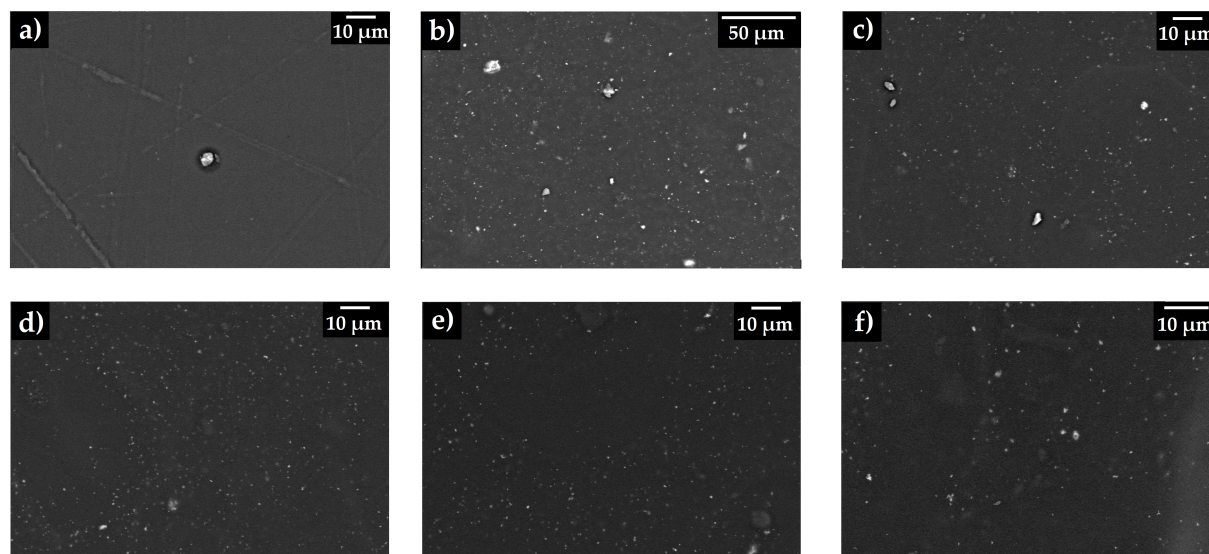


Fig. 2. SEM micrographs of chitosan/potato-starch films, a) control film C, b) film with non-functionalized NPs (T) and films with silanized NPs, c) 1-M1-CPS, d) 1-M2-CPS, e) 1-M3-CPS and f) 1-M4-CPS.

Water activity (a_w) is a critical parameter for microbial growth (Martuscelli *et al.*, 2017). The increase of the a_w is not feasible, since it promotes the deterioration of food (Sánchez-Aldana *et al.*, 2015). The data of a_w of film C and films with TiO_2 are shown in Table 3. The values of this parameter in the films are very similar, but there is a minimum increase of a_w in 1-M4-CPS, which was attributed to the increase in thickness and heterogeneity in the components of the sample, the decrease in concentration of TiO_2 caused that the a_w were similar to the behavior of the polymer sample without NPs. A value of $a_w \leq 0.4$ is considered ideal to avoid microbial proliferation, all samples were maintained between 0.265 and 0.307, with this, the films are considered acceptable for this parameter.

The data of thickness measurements of the films are presented in Table 3. In the absence of functional groups in the TiO_2 , or also, at a very low presence of these, NPs and polymers fail to form hydrogen bonds (Sreekumar *et al.*, 2012), causing that the materials do not have an adequate acceptance and is reflected in an increase in the thickness, this behavior was observed in the film T with 93 μm (20 microns more than the control film). Film samples with TiO_2 modified as 1-M1-CPS, 1-M2-CPS and 1-M3-CPS showed a thickness of 70, 67 and 70 μm respectively, and were similar to film C (73 μm). This behavior of slight decrease in thickness was also observed by Lian *et al.*, (2016) in the incorporation of nano- TiO_2 to films

of polyvinyl alcohol (PVA) and chitosan by high-pressure hydrostatic treatment, the functional groups on the surface of the NPs cause a “compatibility” with the polymer matrix, making the TiO_2 accepted by the film and not increasing the thickness, however, 1-M4-CPS also exhibited an increase in thickness as the film T up to 100 μm due to the non-effective incorporation of the NPs in the film.

In Fig. 2a the micrograph obtained by SEM of the control film C is shown, a smooth surface is observed, the irregularities observed as “lines” are due to the scratches existing in the acrylic plates where the films were poured, while in Fig. 2b shows the film sample with non-functionalized TiO_2 powders (film T), and the NPs are distinguished as light points, and the existence of clusters caused by the agglomeration of these is visualized, as is known from the colloidal tests in aqueous systems (López-Zamora *et al.*, 2018).

The micrographs obtained from the films with silanized NPs are shown in Fig. 2c, the TiO_2 of the film 1-M1-CPS is observed with a better dispersion in the film, however, there are still areas in the sample where there are agglomerations, but in smaller quantity compared with the unmodified powders, while in Fig. 2d, the NPs in 1-M2-CPS also show an effective dispersion, but like the particles of 1-M1-CPS, small clusters of TiO_2 are observed.

The attraction of the TiO_2 particles is due to the attractive forces of Van der Waals, as they do not present repulsion charges on the surfaces

of the particles, they tend to collide and form agglomerates. The micrograph of Fig. 2d shows the surface of the film 1-M3-CPS, good dispersion, but there is still a presence of conglomerates, however, in Fig. 2f, the film 1-M4-CPS is very noticeable since the particles form larger accumulations than the previous micrographs, because the representative sample contains the TiO₂ powders with minor proportions of APTES, these samples were the most similar to the NPs without modification, since they presented less amount of coating by the agent coupling (López-Zamora *et al.*, 2018).

Lian *et al.*, (2016) observed in the micrographs TiO₂ particles and clusters of these on the surfaces of their polyvinyl alcohol-chitosan films that appeared as light points, and some of their samples had transitions between the components of the mixture and the lower layer. It was not smooth. In the micrographs of the samples with NPs, obtained in this research it is possible to appreciate some species of spots and they were attributed to the ineffective dispersion that the chitosan had at the time of the formation of the sol.

Because one of the most important parameters in the application of polymeric films is the tensile strength, since they are used as packaging material, it had been decided to perform an analysis of the effect of the number of particles inside the plastic films. Considering that the M3 particle is the one that showed a higher tensile strength within all the functionalized particles evaluated at 1% w/w with respect to the film-forming materials. In addition, these particles showed a marked improvement in colloidal stability in acid medium during the mixing stage, as we presented in a previous investigation (López-Zamora *et al.*, 2018).

In addition to these characterizations, the photocatalytic degradation or also called photo-oxidation of the films was analyzed. The samples were exposed to UV light for 1,008 hours. Photocatalysis causes the chemical decomposition of compounds, formation of free radicals (Forsthuber *et al.*, 2014) and consequently the degradation of the material. Infrared analyzes were performed on the samples during the exposure to UV light. In Fig. 3, the IR spectra of the films are presented at three different times, it was observed that at 384 h, the intensity of the band caused by the hydroxyl group (-OH) between 3680 and 2999 cm⁻¹ decreased due to the loss of moisture in the samples due to exposure to UV light, as well as the intensities of the other peaks, and this was attributed to the partial breakage of intermolecular and intramolecular hydrogen bonds, as reported by Bajer and Kaczmarek *et al.* (2010). At the wavenumber

approximating 3740 cm⁻¹ small peaks emerged, also attributed to the -OH group (Almazán-Sánchez *et al.*, 2015). Photo-oxidation processes of polymeric species such as chitosan leads to the formation of hydroxyl and carbonyl groups (Vallejo-Montesinos *et al.*, 2017) (at 3740 cm⁻¹ and 1730 cm⁻¹ respectively) on the surface of the film. It should be noted that the spectra of films with silanized TiO₂ are still “soft” curves unlike the control film C and the film T, the latter being the most affected by UV light.

The samples received the radiation for 1008 h and described a pattern in the peaks and bands with less intensity than in the previous time, which indicated the degradation of the material (Forsthuber *et al.*, 2014) in addition to the amino groups in 1580 cm⁻¹ and the group C=O at 1730 cm⁻¹ (carbonyl) changed to higher wave numbers (1650 cm⁻¹ and 1750 cm⁻¹) because the hydrogen bonds formed between the polymers suffered ruptures, which may reduce the crystallinity of polymers (Bajer and Kaczmarek, 2010), as well as the formation of such polar groups (carbonyl and hydroxyl) induced by UV light, is identified by the increase and/or decrease in the ratio between the characteristic peaks of glycosidic bonds and amines (Praxedes *et al.*, 2012).

Despite the exposed time, the curves denote the characteristic peaks of the polymers, however, the most affected film is the sample T, since the photocatalytic effect of the non-functionalized TiO₂ affected the bands and peaks of the region between 3700 to 1900 cm⁻¹, in addition to that the intensity of the major peaks was drastically reduced as reported in the literature (Praxedes *et al.*, 2012, Bajer and Kaczmarek, 2010). All these results indicate that the APTES organic groups influence the reduction of photo-oxidation processes of TiO₂, which gives us a film that, when exposed to UV light, will resist oxidative changes more than one that is only composed of the formation polymers or with TiO₂ without silanizar, since APTES induces a passivation effect to TiO₂.

Regardless of the colorimetry study of the films presented in Table 3, a comparison was made of the changes of the parameters L, a* and b* at the end of the radiation with UV light, these data are shown in Table 4.

All the films decreased in luminosity at the end of the photo-oxidation processes, that is, the samples were darker compared to the initial time, 1-M3-CPS had the highest value, followed by film T, while for the coordinate a* only the film C and 1-M2-CPS remained in values of the green region, although they decreased,

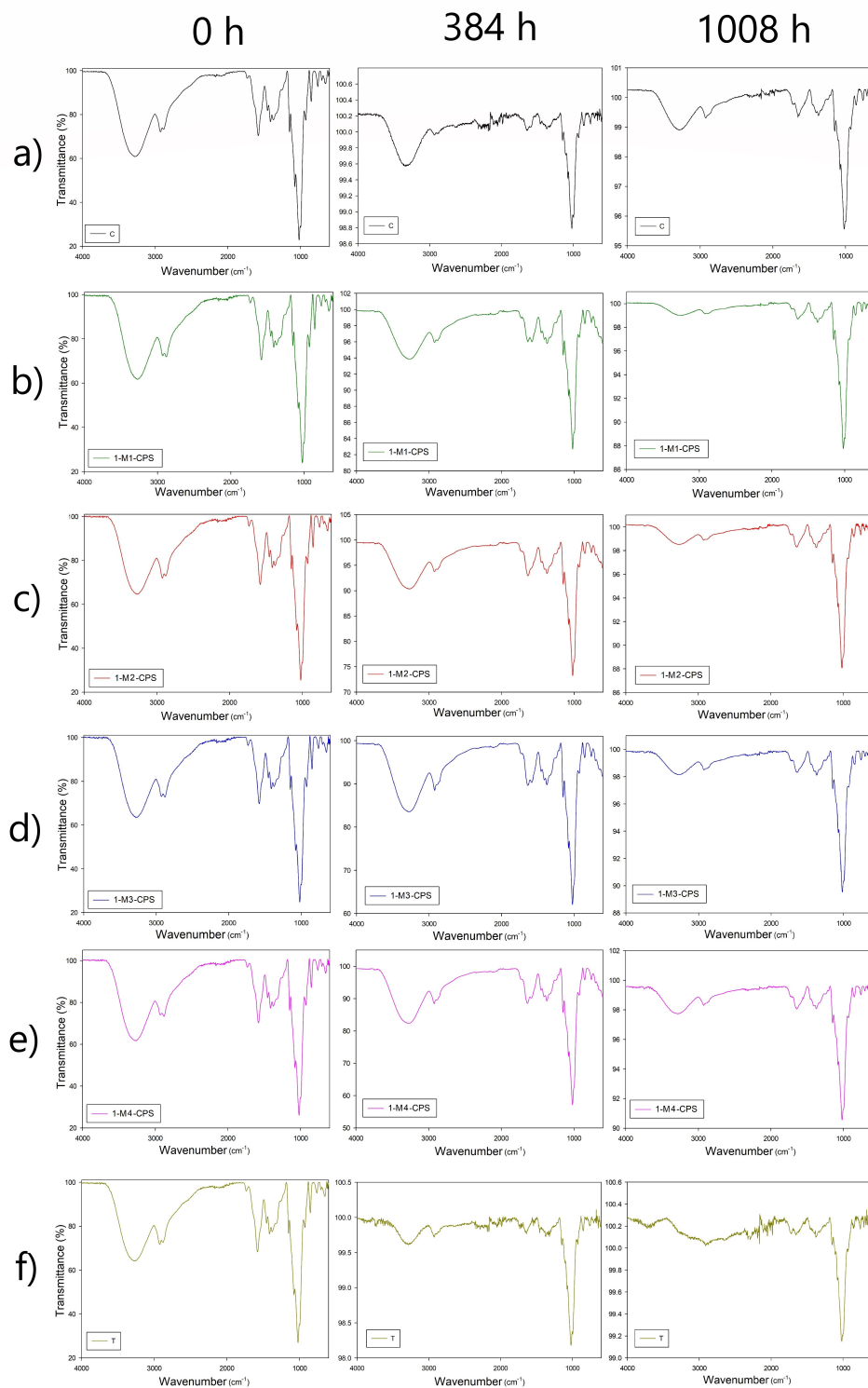


Fig. 3. Infrared spectra of exposure to UV light of 0, 384 and 1008 h of the films: a) Control film C, b) 1-M1-CPS, c) 1-M2-CPS, d) 1-M3-CPS, e) 1-M4-CPS and f) film T.

Table 4. Colorimetric analysis of the photo-oxidation process of the films, t_0 = before UV exposure, t = after 1008 h of UV light.

| Sample | L (t_0) | L (t) | a* (t_0) | a* (t) | b* (t_0) | b* (t) |
|-----------------|-------------|-----------|--------------|------------|--------------|------------|
| C | 30.51 | 12.05 | -0.17 | -0.73 | 1.43 | 3.3 |
| T | 51.22 | 27.75 | -2.17 | 1.91 | 2.56 | 12.07 |
| 1-M1-CPS | 51.58 | 26.37 | -2.35 | 0.25 | 2.83 | 9.14 |
| 1-M2-CPS | 49.73 | 24.65 | -2.1 | -0.26 | 1.1 | 8.66 |
| 1-M3-CPS | 48.08 | 28.46 | -1.9 | 0.81 | 1.4 | 10.79 |
| 1-M4-CPS | 45.93 | 23.61 | -1.71 | 0.17 | 2.32 | 8.94 |

Table 5. Colorimetry, a_w , thickness and mechanical properties of the chitosan/potato-starch films with change of load of TiO₂ (0.5% and 0.1% w/w).

| Sample | a_w | L | a* | b* | Thickness (μm) | Young's modulus (MPa) | Tensile strength (MPa) | Elongation at break (%) |
|-------------------|-------|-------|-------|------|-----------------------------|-----------------------|------------------------|-------------------------|
| T | 0.27 | 51.22 | -2.17 | 2.56 | 93 | 348.13 | 20.76 | 37 |
| 1-M3-CPS | 0.29 | 48.08 | -1.9 | 1.4 | 70 | 237.96 | 18.06 | 45 |
| 0.5-T-CPS | 0.27 | 42.36 | -1.48 | 1.99 | 67 | 180.4 | 18.37 | 43 |
| 0.5-M3-CPS | 0.27 | 45.05 | -1.85 | 2.91 | 87 | 236.6 | 22.35 | 54 |
| 0.1-T-CPS | 0.27 | 33.55 | -0.38 | 1.7 | 70 | 428.33 | 24.06 | 36 |
| 0.1-M3-CPS | 0.28 | 33.12 | -0.46 | 1.8 | 70 | 373.2 | 16.55 | 18 |

while the other samples had a redshift, finally, in the b^* parameter, the samples indicated an increase in the yellow color. Summarizing these data, the loss of whiteness, the displacement to a reddish color and the yellowing of the film, indicate a color similar to sepia at the end of the UV exposure period.

3.2 Effect of the amount of filler on the properties of chitosan/potato-starch films

The films made with the M3 particles show a better performance in the resistance to the loss of luminosity, in addition to using a small amount of APTES to carry out the chemical modification of TiO₂, for what is considered that these particles are a good option to be used as a filler. It has also been shown that the M3 particles have a good stability at acidic pH values, which are used in the formation of the FFS, so that this particle inside the film was studied considering a change in the load of nanoparticles to observe the effects produced when incorporating them in the films and compare them with the NPs without functionalizing. Table 5 presents the results obtained.

For the samples with different concentrations of NPs there was an increase in the thickness (0.5-M3-CPS) probably due to the little formation of bonds between the polymers and the TiO₂, while the others maintain a thickness similar to the film

of chitosan/potato-starch. For the water activity, the values were similar to the control film, this probably due to the lower amount of functionalized TiO₂, since the hydroxyl groups of the surface, or the organic groups of the APTES, could form smaller hydrogen bonds and lower moisture uptake, but it is practically very small unlike its counterparts at 1% w/w.

For the mechanical tests, the decrease to 0.5% by weight of the concentration of the NPs in the films caused a different effect, and this is observed in the data in Table 5. In these concentrations, the sample 0.5-M3-CPS with functionalized TiO₂ showed values greater than 0.5-T-CPS, the opposite of its counterparts at 1%, where the Young's modulus and the tensile strength of the films decreased with the presence of APTES. If you compare the data of 0.5-M3-CPS with those of 1-M3-CPS, they are very close, even the data are better balanced, since it has a greater elongation than the one of the load of 1%, however this behavior it does not prevail when the concentration decreases to 0.1% by weight in films. For the sample 0.1-T-CPS, the modulus of elasticity increases drastically, surpassing any value analyzed in this work, the above is attributed to the fact that the particles of TiO₂ are in a sufficiently small proportion to avoid the formation of agglomerates. Finally, 0.1-M3-CPS also showed an increase only of module and TS, since the elongation was very poor, making the film very brittle and having an immediate break in the tensile tests.

According to our study, it was observed in the infrared spectroscopy and X-ray scattering tests that the different functionalization routes of the NPs do not affect the patterns of these techniques, this information is shown in the supplementary material.

Conclusions

The introduction of nanometric particles of TiO₂ to chitosan/potato-starch films caused changes in optical, mechanical and thermal properties. The presence of functional groups of the APTES coupling agent on the surface of the TiO₂ NPs also influenced the results of all the data collected. The films increased in luminosity due to the pigmentation of the NPs, the aw remained practically close to the control, remaining within the acceptable values for microbial nonproliferation, concluding that the APTES does not significantly influence this parameter. The thermal analysis indicated that the addition of TiO₂ increases the glass transition temperature in the film, but that the addition of functional groups such as those of APTES, gives mobility to the polymer chains at the time of temperature rise, causing the necessary temperature is lower to leave a vitreous state, the most important thing was that the existence of these functional groups reduced the enthalpy of decomposition of the films making them more stable at the time of thermal degradation compared to the film with NPs without APTES. The coupling agent and the bonds that formed between the polymer chains also modified the results of the mechanical tests, the behaviors shown by the films with silanized NPs had better balanced properties than the control film C and film T, since they increased their elongation without sacrificing in an excessive way its tensile strength, the peculiar thing was that by decreasing the load of NPs, the behavior of the samples was different, since 0.5-M3-CPS showed better values than its counterpart at 1%, in this behavior it is attributed the influence of its thickness a little greater than its counterpart, as well as the compatibility and formation of bonds between the polymers and TiO₂, and the effective dispersion of TiO₂ was visualized in the micrographs, also being appreciated in the thickness. The effect of the photo-oxidation was reflected in the final color, since from white they became a color similar to sepia or brown, according to our analysis. The photo-oxidation results suggested the passivation of TiO₂ thanks to APTES, which implies that it is a more

stable film against UV radiation, avoiding the negative effect of TiO₂ particles without modifying; this could be due to the hydrophilic nature of the films, they bind to the particles on the outside (amino groups), thus causing the electron movement to take place in the hydrophobic part (siloxane). Improving the photocatalytic stability of the particles and avoiding photodegradation.

Acknowledgements

The authors express their gratitude to Professor Georgette Kay Kerr for the english language editing, Claudia Elias Alfaro for experimental assistance in the TEM measurements and to Tecnológico Nacional de Mexico for the Grant by the "Support to Infrastructure and Research" program with the projects 6338.17-P (L. Lopez-Zamora) and 6409.18-P (J.A. Gonzalez-Calderon).

References

- Ahmad A., Razali M. H., Mamat M., Mehamod F. S. B., Amin K. A. M. (2017). Adsorption of methyl orange by synthesized and functionalized-CNTs with 3-aminopropyltriethoxysilane loaded TiO₂ nanocomposites. *Chemosphere* 168, 474-482.
- Almazan-Sánchez P. T., Catañeda-Juárez M., Martínez-Miranda V., Solache-Ríos M., Lugo-Lugo V., Linares-Hernández I. (2015). Behavior of TOC and color in the presence of iron-modified activated carbon in methyl methacrylate wastewater in bath and column systems. *Water Air Soil Pollution* 226, 1-13.
- Arockianathan P.M. Sekar S. Kumaran B. Sastry T.P. (2012). Preparation, characterization and evaluation of biocomposite films containing chitosan and sago starch impregnated with silver nanoparticles. *International Journal Biological Macromolecules* 50, 939-946.
- Bajer D., Kaczmarek H. (2010). Study of the influence OV UV radiation on biodegradable blends based on chitosan and starch. *Progress on Chemistry and Application of Chitin and its Derivatives* 15, 17-24.
- Bergel B. F., da Luz L.M., Santana R. M.C. (2017). Comparative study of the influence of chitosan as coating of thermoplastic starch foam from

- potato, cassava and corn starch. *Progress in Organic Coatings* 106, 27-32.
- Bourtoom T., Chinnan M. S. (2008). Preparation and properties of rice starch-chitosan blend biodegradable film. *LWT-Food Science and Technology* 41, 1633-1641.
- Bozzi A., Yuranoza T., Guasaquillo I., Laub D., Kiwi J. (2005). Self-cleaning of modified cotton textiles by TiO₂ at low temperatures under daylight irradiation. *Journal of Photochemistry and Photobiology A: Chemistry* 174, 156-164.
- Chakrabarty T., Kumar M., Shahi V.K. (2010). Chitosan based membranes for separation, pervaporation and fuel cell applications: Recent developments In: *Biopolymers* (Elnashar M.M. eds). Pp 201-226. SCIYO, Rijeka, Croatia
- Dang K. M., Yoksan R. (2016). Morphological characteristics and barrier properties of thermoplastic starch/chitosan blown film. *Carbohydrate Polymers* 150, 40-77.
- Daoud W. A., Xin J. H., Zhang Y.H. (2005). Surface functionalization of cellulose fibers with titanium dioxide nanoparticles and their combined bactericidal activities. *Surface Science* 599, 69-75.
- Dhawade P. P., Jagtap R.N. (2012). Characterization of the glass transition temperature of chitosan and its oligomers by temperature modulated differential scanning calorimetry. *Advances in Applied Science Research* 3, 1372-1382.
- Dias A. B., Müller C. M. O., Larotonda F. D. S., Laurindo J. B. (2010). Biodegradable films based on rice starch and rice flour. *Journal of Cereal Science* 51, 213-219.
- Estrada-Monje, A., Andreu-Díaz, J. M., Cruz-Salgado, J. (2016). Películas de ldpe/nano-TiO₂ con propiedades antibacteriales inducidas por ultrasonido. *Revista Mexicana de Ingeniería Química* 15, 953-960.
- Forsthuber B., Müller U., Teischinger A., Grüll G. (2014). A note on evaluating the photocatalytic activity of anatase TiO₂ during photooxidation of acrylic clear Wood coatings by FTIR and mechanical characterization. *Polymer Degradation and Stability* 105, 206-210.
- Furuzono T., Iwasaki M., Yasuda S., Korematsu A., Yoshioka T., Ito S., Kishida A. (2003). Photoreactivity and cell adhesiveness of amino-group-modified titanium dioxide nano-particles on silicone substrate coated by covalent linkage. *Journal of Materials Science Letters* 22, 1737-1740.
- Hadi-Najafabadi H., Irani M., Roshanferk-Rad L., Heydari-Haratameh A., Haririan I. (2015). Removal of Cu²⁺, Pb²⁺ and Cr⁶⁺ from aqueous solutions using a chitosan/graphene oxide composite nanofibrous adsorbent. *RSC Advances* 5, 16532-16539.
- Hamden Z., Bouattour S., Ferraria A. M., Ferreira D. P., Vieira-Ferreira L. F., Botelho do Rego A. M., Boufi S. (2016). *In situ* generation of TiO₂ nanoparticles using chitosan as a template and their photocatalytic activity. *Journal of Photochemistry and Photobiology A: Chemistry* 321, 211-222.
- Hamdi A., Boufi S., Bouattour S. (2015). Phthalocyanine/chitosan-TiO₂ photocatalysts: Characterization and photocatalytic activity. *Applied Surface Science* 339, 128-136.
- Hari N., Nair A. J. (2016). Development and characterization of chitosan-based antimicrobial films incorporated with streptomycin loaded starch nanoparticles. *New Horizons in Translational Medicine* 3, 22-29.
- Huang S., Guild B., Neethirajan S., Therrien P., Lim L.T., Warriner K. (2017) Antimicrobial coatings for controlling *Listeria monocytogenes* based on polylactide modified with titanium dioxide and illuminated with UV-A. *Food Control* 73, 421-425.
- Jiang S., Liu C., Wang X., Xiong L., Sun Q. (2016). Physicochemical properties of starch nanocomposite films enhanced by self-assembled potato starch nanoparticles. *LWT-Food Science and Technology* 69, 251-257.
- Kimura V. T., Miyasato C.S., Genesi B.P., Lopes P.S., Yoshida C. M.P., da Silva C.F. (2016). The effect of andiroba oil and chitosan concentration on the physical properties of chitosan emulsion film. *Polímeros* 26, 168-175.

- Li B., Zhang Y., Yang Y., Qui W., Wang X., Liu B., Wang Y., Sun G. (2016). Synthesis, characterization, and antibacterial activity of chitosan/TiO₂ nanocomposites against *Xanthomonas oryzae*. *Carbohydrate Polymers* 152, 825-831.
- Lian Z., Zhang Y., Zhao Y. (2016). Nano-TiO₂ particles and high hydrostatic pressure treatment for improving functionality of polyvinyl alcohol and chitosan composite films and nano-TiO₂ migration from film matrix in food simulants. *Innovative Food Science and Emerging Technologies* 33, 145-153.
- Liu L., Mei A., Liu T., Jiang P., Sheng Y., Zhang L., Han H. (2015). Fully printable mesoscopic perovskite solar cells with organic silane self-assembled monolayer. *Journal of the American Chemical Society* 137, 1790-1793.
- López-Chavez, M. C., Osorio-Revilla, G., Arellano-Cárdenas, S., Gallardo-Velázquez, T., Flores-Valle, S. O., López-Cortez, M. S. (2017). Preparation of starch/clay/glycerol nanocomposite films and their FTIR, XRD, SEM and mechanical characterizations. *Revista Mexicana de Ingeniería Química* 16, 793-804.
- López-Zamora L., Martínez-Martínez H. N., González-Calderón J. A. (2018). Improvement of the colloidal stability of titanium dioxide particles in water through silicon based coupling agent. *Materials Chemistry and Physics* 217, 285-290.
- Martuscelli M., Lupieri L., Sacchetti G., Mastrocola D., Pittia P. (2017). Prediction of the salt content from water activity analysis in dry-cured ham. *Journal of Food Engineering* 200, 29-39.
- Mei J., Yuan Y., Wu Y., Li Y. (2013). Characterization of edible starch-chitosan film and its application in the storage of Mongolian cheese. *International Journal of Biological Macromolecules* 57, 17-21.
- Meroni D., Lo Presti L., Di Liberto G., Ceotto M., Acres R. G., Prince K. C., Bellani R., Soliveri G., Ardizzone S. (2017). A close look at the structure of the TiO₂-APTES interface in hybrid nanomaterials and its degradation pathway: An experimental and theoretical study. *The Journal of Physical Chemistry C* 121, 430-440.
- Mihailović D., Šaponjić Z., Radoičić M., Radetić T., Jovančić P., Nedeljković J., Radetić M. (2010). Functionalization of polyester fabrics with alginates and TiO₂ nanoparticles. *Carbohydrate Polymers* 79, 526-532.
- Ochoa Y., Ortegón Y., Rodríguez-Páez J. E. (2010). Síntesis de TiO₂, fase anatasa, por el método sol-gel: estudio de la presencia de AcacH en el sistema. *Grupo de Ciencia y Tecnología de Materiales Cerámicos* 52, 29-40.
- Oleyaei S.A., Zahedi Y., Ghanbarzadeh B., Moayedi A. A. (2016). Modification of physicochemical and thermal properties of starch films by incorporation of TiO₂ nanoparticles. *International Journal of Biological Macromolecules* 89, 256-264.
- Ostafińska A., Mikešová J., Krejčíková S., Nevoralová M., Štuncová A., Zhigunov A., Michálková D., Šlouf M. (2017). Thermoplastic starch composites with TiO₂ particles: Preparation, morphology, rheology and mechanical properties. *International Journal of Biological Macromolecules* 101, 273-282.
- Ostwal M., Singh R. P., Dec S. F., Lusk M. T., Way J. D. (2011). 3-Aminopropyltriethoxysilane functionalized inorganic membranes for high temperature CO₂/N₂ separation. *Journal of Membrane Science* 369, 139-147.
- Perez J. J., Francois N. J. (2016). Chitosan-starch beads prepared by ionotropic gelation as potential matrices for controlled release of fertilizers. *Carbohydrate Polymers* 148, 134-142.
- Praxedes A. P. P., da Silva A. J. C., da Silva R. C., Lima R. P.A, Tonholo J., Ribeiro A. S., de Oliveira I. N. (2012). Effects of UV irradiation on the wettability of chitosan films containing dansyl derivatives. *Journal of Colloid and Interface Science* 376, 255-261.
- Razzaz A., Ghorban A., Hosayni L., Irani M., Aliabadi M. (2016). Chitosan nanofibers functionalized by TiO₂ nanoparticles for the removal of heavy metal ions. *Journal of the Taiwan Institute of Chemical Engineers* 58, 333-343.
- Sánchez-Aldana D., Contreras-Esquivel J.C., Nevárez-Moorillón G. V., Aguilar C. N. (2015).

- Caracterización de películas comestibles a base de extractos pécticos y aceite esencial de limón mexicano. *CyTA-Journal of Food* 13, 17-25.
- Santacruz S., Rivadeneira C., Castro M. (2015). Edible films based on starch and chitosan. Effect of starch source and concentration, plasticizer, surfactant's hydrophobic tail and mechanical treatment. *Food Hydrocolloids* 49, 89-94.
- Sarwar A., Katas H., Samsudin S. N., Zin N. M. (2015). Regioselective Sequential modification of chitosan via azide-alkyne click reaction: Synthesis, characterization, and antimicrobial activity of chitosan derivatives and nanoparticles. *PLoS ONE* 10, e0123084, 1-22
- Shiraishi, F., Ueno, M., Chand, R., Shibata, Y., Luitel, H. N. (2014). Effect of silanization of titanium dioxide on photocatalytic decomposition of 2,4-dinitrophenol under irradiation with artificial UV light and sunlight. *Journal of Chemical Technology and Biotechnology* 89, 81-87.
- Shirakawa M. A., John V. M., Mocelin A., Zilles R., Toma S. H., Araki K., Toma H. E., Thomaz A. C., Gaylarde C. C. (2016). Effect of silver nanoparticle and TiO₂ coatings on biofilm formation on four types of modern glass. *International Biodeterioration and Biodegradation* 108, 175-180.
- Silva-Pereira M. C., Teixeira J. A., Pereira-Júnior V. A., Stefani R. (2015). Chitosan/corn starch blend films with extract from Brassica oleraceae (red cabbage) as a visual indicator of fish deterioration. *Food Science and Technology* 61, 258-262.
- Silva-Weiss A., Bifani V., Ihl M., Sobral P. J. A. y Gómez-Guillén M. C. (2013). Structural properties of films and rheology of film-forming solutions based on chitosan and chitosan-starch blend enriched with murta leaf extract. *Food Hydrocolloids* 31, 458-466.
- Solís-Gómez A., Neira-Velázquez M. G., Morales J., Sánchez-Castillo M. A., Pérez E. (2014). Improving stability of TiO₂ particles in water by RF-plasma polymerization of poly(acrylic acid) on the particle surface. *Colloids and Surfaces A: Physicochemical and Engineering Aspects* 451, 66-74.
- Soto-Borbón, M. A., Sánchez-Corrales, V. M., Trujillo-Camacho, M. E. (2014). Characterization of TiO₂/alginate screenprinting films. *Revista Mexicana de Ingeniería Química* 13, 227-236.
- Sreekumar P.A., Al-Harthi M. A., De S. K. (2012). Reinforcement of starch/polyvinyl alcohol blend using nano-titanium oxide. *Journals of Composite Materials* 46, 3181-3187.
- Tripathi S., Mehrotra G. K. y Dutta P. K. (2009). Physicochemical and bioactivity of cross-linked chitosan-PVA film for food packaging applications. *International Journal of Biological Macromolecules* 45, 372-376.
- Vallejo-Montesinos J., López-Martínez J. C., Montejano-Carrizales J. M., Pérez E., Balcázar-Pérez J., Almendárez-Pérez A., González-Calderon J. A. (2017). Passivation of titanium oxide in polyethylene matrices using polyelectrolytes as titanium dioxide surface coatings. *Mechanics, Materials Science and Engineering* 8, doi: 10.2412/mmse.96.48.950
- Vásconez M. B., Flores S. K., Campos C. A., Alvarado J., Gerschenson L. N. (2009). Antimicrobial activity and physical properties of chitosan-tapioca starch based edible films and coatings. *Food Research International* 42, 762-769.
- Volpe S., Cavella S., Masi P., Torrieri E. (2017). Effect of solid concentration on structure and properties of chitosan-caseinate blend films. *Food Packaging and Shelf Life* 13, 76-84.
- Weerachawanasak P., Hutchings G. J., Edwards J. K., Kondrat S. A., Miedziak P. J., Praserttham P., Panpranot J. (2015). Surface functionalized TiO₂ supported Pd catalysts for solvent-free selective oxidation of benzyl alcohol. *Catalysis Today* 250, 218-225.
- Xiao G., Zhang X., Zhang W., Zhang S., Su H., Tan T. (2015). Visible-light-mediated synergistic photocatalytic antimicrobial effects and mechanism of Ag-nanoparticles chitosan-TiO₂ organic-inorganic composites for water disinfection. *Applied Catalysis* 170-171, 255-262.
- Xu Y. X., Kim K. M., Hanna M. A. y Nag D. (2005). Chitosan-starch composite film: preparation and

- characterization. *Industrial Crops and Products* 21,185-192.
- Zarazua-Aguilar, Y., Paredes-Carrera, S. P., Sánchez-Ochoa, J. C., Avendãno-Gómez, J. R., Flores-Valle, S. O. (2017). Influencia de la irradiación microondas/ultrasonido en la síntesis sol-gel de nano partículas de dióxido de titanio para su aplicación en fotocatalisis. *Revista Mexicana de Ingeniería Química* 16, 899-909.
- Zhai M., Zhao L., Yoshii F., Kume T. (2004). Study on antibacterial starch/chitosan blend film formed under the action of irradiation. *Carbohydrate Polymers* 57, 83-88.
- Zhang W., Chen J., Chen Y., Xia W., Xiong Y. L., Wang H. (2016). Enhanced physicochemical properties of chitosan/whey protein isolate composite film by sodium laurate-modified TiO₂ nanoparticles. *Carbohydrate Polymers* 138, 59-65.
- Zhou M., Liu Q., Wu S., Gou Z., Wu X., Xu D. (2016). Starch/chitosan films reinforced with polydopamine modified MMT: Effects of dopamine concentration. *Food Hydrocolloids* 61, 678-684.